# Using improved particle swarm optimization to tune PID controllers in cooperative collision avoidance systems[*]

Xing-chen WU[1], Gui-he QIN[1,2], Ming-hui SUN[†‡1,2], He YU[3], Qian-yi XU[1]

(*[1]College of Computer Science and Technology, Jilin University, Changchun 130012, China*)
(*[2]MOE Key Laboratory of Symbol Computation and Knowledge Engineering, Changchun 130012, China*)
(*[3]Department of Measurement and Controlling Engineering, Changchun University, Changchun 130012, China*)
[†]E-mail: 511518984@qq.com

**Abstract:** The introduction of proportional-integral-derivative (PID) controllers into cooperative collision avoidance systems (CCASs) has been hindered by difficulties in their optimization and by a lack of study of their effects on vehicle driving stability, comfort, and fuel economy. In this paper, we propose a method to optimize PID controllers using an improved particle swarm optimization (PSO) algorithm, and to better manipulate cooperative collision avoidance with other vehicles. First, we use PRESCAN and MATLAB/Simulink to conduct a united simulation, which constructs a CCAS composed of a PID controller, maneuver strategy judging modules, and a path planning module. Then we apply the improved PSO algorithm to optimize the PID controller based on the dynamic vehicle data obtained. Finally, we perform a simulation test of performance before and after the optimization of the PID controller, in which vehicles equipped with a CCAS undertake deceleration driving and steering under the two states of low speed (≤50 km/h) and high speed (≥100 km/h) cruising. The results show that the PID controller optimized using the proposed method can achieve not only the basic functions of a CCAS, but also improvements in vehicle dynamic stability, riding comfort, and fuel economy.

**Key words:** Cooperative collision avoidance system (CCAS); Improved particle swarm optimization (PSO); PID controller; Vehicle comfort; Fuel economy

## 1 Introduction

With the increase in the number of automobiles, the number of road accidents exhibits an upward tendency. Hence, the study on how to improve traffic safety becomes significant. As a vehicle initiative safety technique that can be adopted to reduce the traffic accident rate, cooperative collision avoidance systems (CCASs) play an important role in cutting down rear-end chain collisions and forward collisions (Seo *et al*., 2014). The emergence of vehicle-to-vehicle (V2V) communication technology makes it

possible for dynamic data interactions among automobiles (Lee *et al.*, 2010). As CCAS, which is generated by combining V2V with collision avoidance systems (CAS), can be used to share location, kinetics, and other information of automobiles in real time, the accuracy of CAS is enhanced to a certain extent. Therefore, CCAS has a broad technical prospect and high practical value. Due to the features of a proportional-integral-derivative (PID) controller, such as structural simplicity, reliability, and convenience for adjustment, it is rational to incorporate the PID controller in the control unit of CCAS (Wang *et al*., 1997). PID controller optimization in accordance with specific environments, as a typical multi-objective optimization problem, is the focus of this study. To solve such a problem, an evolutionary algorithm, which is a global optimization algorithm

with high robustness and general applicability, is employed.

A vast amount of literature on CCAS is available. Zardosht *et al.* (2013) presented a decision-making module for accident situations, which processes information from vehicular ad hoc network communication (VANET). The module can be implemented in each vehicle to assist the driver in certain situations. Wang and Phillips (2013) proposed a path-planning scheme for a multi-agent movement system. They used reinforcement learning to develop a maneuvering decision sequence. Ong and Gerdes (2015) proposed a proximal message passing algorithm to solve the simple model predictive control problems of CCAS. Intersection-collision warning systems that use vehicle-to-infrastructure (V2I) communication to avoid accidents at urban intersections face the problems of real-time information delivery and high cost. Cho and Kim (2014) proposed an intersection-collision warning system based on V2V communication to solve such problems. Tan and Huang (2006) explored the feasibility of cooperative collision warning systems (CCWSs), where vehicles are equipped with a relatively simple differential global positioning system (DGPS) and motion sensors. Yan *et al.* (2010) derived analytical expressions for key CCWS metrics that rely on mobility information exchanged by various players. They analyzed mobility parameters and derived the conditional probability of a collision. To enhance the accuracy of CCWS, Huang and Lin (2014) proposed a vector-based CCWS (VCCW).

Although the vehicle collision avoidance and emergency steering functions of CCAS have been implemented in previous studies, the stability, driving comfort, and fuel economy of vehicles have not been taken fully into account. In addition, when optimized PID controllers are introduced into CCAS, ideal PID controller optimization results cannot be acquired by common genetic algorithms, due to their defects such as prematurity and poor stability. Therefore, the popularization and development of CCAS have been restricted.

To solve these problems, in this study we adopt an improved particle swarm optimization (PSO), which has the characteristics of high precision and ease of convergence, to optimize the performance of CCAS control units. To validate this method, two different types of vehicle equipped with CCAS were used in experiments related to their deceleration steering and braking at low and high cruising speeds, before and after the improved PSO was applied to the PID controller. During these experiments, vehicles kinetic data were acquired, including longitudinal and transverse speeds, accelerations, and longitudinal displacement of tires. Analysis of the data showed that the approach of setting a PID controller using the improved PSO can improve steering stability, driving comfort, and fuel economy of automobiles with CCAS.

## 2 PID controller tuning based on improved PSO

PID calibration is applicable to a CCAS as a lagging controlled object with inertia, because it has the ability to partly decrease system overshoot and rise time, and to improve system stability and rapidity (Feng *et al.*, 2012). As PSO has fast convergence property and simple algorithm structure, and is appropriate for value type processing, it satisfies the optimization requirements of a PID controller in this study. Thus, we adopt a PID controller to improve the dynamic behavior of the CCAS during regulation and PSO to adjust the parameter of the PID controller.

### 2.1 Improved PSO

During the optimization process of PSO, there can be problems such as being trapped into local optima and premature evolutionary stagnation. Jin *et al.* (2010) introduced the worst position for individual and spherical particles in standard PSO. This method not only accelerates the convergence of particles, but also increases the diversity of particles in a group, promoting the global optimality of convergence. Shi and Eberhart (1998; 2001) noted that the global search ability is stronger when $\omega$ is relatively large; otherwise, the local search ability is stronger. Based on this, they proposed the method of random inertia weighting, in which the value of $\omega$ decreases linearly. To increase the diversity of particles in the group, Zhang *et al.* (2008) introduced a random acceleration factor into standard PSO calculation. According to the test, this method improves the local search ability of PSO. In this study, when introducing the worst

positions of individual and spherical particles into standard PSO, we consider the positive effects of random inertia weighting and the random learning factor on the diversity of the particle swarm and on avoiding the trapping into local optima while keeping the convergence rate. To adjust the PID controller using the improved PSO, let $\boldsymbol{k}=[k_v, k_r, k_a]$ represent an individual vector for the particle swarm, where $k_v$, $k_r$, and $k_a$ represent proportion, integration, and differentiation, respectively. The particle swarm consisted of 10 particles. Therefore, the maximum search space $d$ was 30. The velocity and position of particle $i$ can be calculated by

$$\begin{aligned} \boldsymbol{v}_i(t+1) = {} & \omega(t)\boldsymbol{v}_i(t) \\ & +c_1 r_1(\boldsymbol{P}_i - \boldsymbol{k}_i(t)) - \sigma_1 r_1(\boldsymbol{P}_i' - \boldsymbol{k}_i(t)) \\ & +c_2 r_2(\boldsymbol{P}_g - \boldsymbol{k}_i(t)) - \sigma_2 r_2(\boldsymbol{P}_g' - \boldsymbol{k}_i(t)), \end{aligned} \quad (1)$$

$$\boldsymbol{k}_i(t+1) = \boldsymbol{k}_i(t) + \boldsymbol{v}_i(t+1), \quad (2)$$

$$\omega(t) = \omega_{\max} - \frac{\omega_{\max} - \omega_{\min}}{t_{\max}}t, \quad (3)$$

where $t$ corresponds to the iteration index, $\boldsymbol{v}_i(t)$ the current velocity of particle $i$, and $\boldsymbol{v}_i(t+1)$ the next stage velocity. $\boldsymbol{P}_i$ is the optimal position of particle $i$ during the current search, and $\boldsymbol{P}_g$ is the optimal position of the particle swarm during the current search. To describe the effects of the individual and global worst values on the update process of a particle's velocity, we introduce $\sigma_1$ and $\sigma_2$, which are uniformly distributed in $[1.8, 2.0]$ as dynamic response factors (Jin *et al.*, 2010). $\boldsymbol{P}_i'$ and $\boldsymbol{P}_g'$ correspond to the positions where particle $i$ and the particle swarm have the worst solutions, respectively. According to Zhang *et al.* (2008), we introduce two random acceleration factors $c_1$ and $c_2$, which are random numbers uniformly distributed in $[1.8, 2.0]$ and remain unchanged during the swarm initialization. $r_1$ and $r_2$ are random numbers distributed in $[0, 1]$. $\boldsymbol{k}_i(t)$ and $\boldsymbol{k}_i(t+1)$ represent current and next locations of particle $i$, respectively. The inertia weight $\omega$ decreases linearly with the number of iterations (Eq. (3)). In this study, the maximum and minimum inertia weights $\omega_{\max}$ and $\omega_{\min}$ were 1.2 and 0.4, respectively. $t_{\max}$ stands for the maximum iteration number of PSO and was 100 in this study.

## 2.2 PID controller tuning

In this study, the outputs of the accelerating and decelerating pedals are used to indicate the final objective function. Based on Kreuzen (2012), we propose a corresponding PID control rate to apply the modified PSO to PID control:

$$\begin{aligned} u_{\mathrm{PID}}(\boldsymbol{K}) = {} & k_r(r_{\mathrm{ept}}(\boldsymbol{K}) - r(\boldsymbol{K})) + k_v(v_{\mathrm{ept}}(\boldsymbol{K}) - v(\boldsymbol{K})) \\ & +k_a(a_{\mathrm{ept}}(\boldsymbol{K}) - a(\boldsymbol{K})), \end{aligned} \quad (4)$$

where $v_{\mathrm{ept}}(\boldsymbol{K})$, $a_{\mathrm{ept}}(\boldsymbol{K})$, and $r_{\mathrm{ept}}(\boldsymbol{K})$ are the expected dynamic statuses of the vehicle. $v(\boldsymbol{K})$, $a(\boldsymbol{K})$, and $r(\boldsymbol{K})$ are the actual dynamic statuses of the vehicle. $r(\boldsymbol{K})$ and $a(\boldsymbol{K})$ stand for the integration and differentiation of $v(\boldsymbol{K})$, respectively. A controlled variable is set up from the linear combination of the deviation between the vehicle's practical and expected dynamic states according to the above parameters, and the performance of the CCAS control unit can be improved.

The optimization of the PID controller involves determining appropriate $k_a$, $k_v$, and $k_r$ values to optimize the performance of the CCAS control unit with the objective that all the integrated evaluation indicators and certain rules are satisfied. To increase the optimization efficiency, we first confirm the upper and lower bounds for searching for the parameters of the PID controller using the Zieglar-Noeols (ZN) method. The introduced error property index $J$ should be minimized for the stability and robustness of the optimized PID controller. Here, we introduce the integrated square error (ISE) as the error property index:

$$J = \int_0^\infty e^2(t)\mathrm{d}t, \quad (5)$$

where $e$ is the error function.

Based on the conditions above, we initialize a 10-particle swarm, in which each particle works as a feasible solution. The velocity, acceleration, and distance of the vehicle under the simulation environment are used as input. Based on the evaluation function, parameters $k_a$, $k_v$, and $k_r$ are optimized in the setting range using the modified PSO. The fitting parameters for the PID controller are found after 100 iterations.

To test the effectiveness of the proposed method, we conducted a step response test using the original PID controller and the PID controller optimized by

the modified PSO (Fig. 1). The obtained optimal values of the PID controller are $k_v=1.8882$, $k_r=-1.0281$, and $k_a=0.5980$. As shown in Fig. 1, the rising time of the PID controller optimized by the improved PSO is shorter than those of the original PID controller and the PID controller optimized by standard PSO. Meanwhile, the overshoot of the PID controller optimized by the improved PSO is obviously smaller than those of the original PID controller and the PID controller optimized by standard PSO. Thus, we can infer that the PID controller optimized by the modified PSO can better access the state of stability.
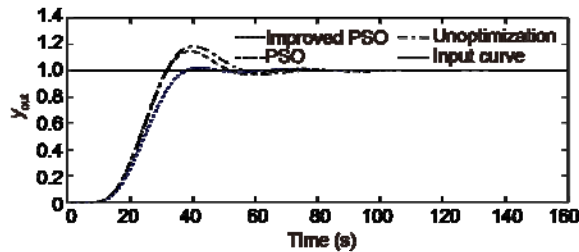


**Fig. 1  Step response of the closed-loop PID controller**

When the vehicle is driving at a relatively low or high speed, the methods of deceleration braking and deceleration steering maneuvering are the most effective in avoiding crashes with target vehicles. Based on Solyom and Bengtsson (2012), we used the vehicle velocity judgment threshold $v$ in Eq. (6) to decide which maneuvering method to choose in the particular cases in our study:

$$v = 2a\sqrt{\frac{w}{y''}}, \qquad (6)$$

where $v$ is the vehicle velocity judgment threshold, $w$ the lateral deviation for the vehicle to avoid crash with the target vehicles or barriers, and $a$ and $y''$ the acceleration and lateral acceleration of the vehicle, respectively.

When the vehicle avoids a crash with a target vehicle by adopting deceleration steering maneuvering, an important component of the CCAS is a reasonable turning path planning model to improve the dynamic stability and riding comfort of the vehicle. According to related studies, when the driver adopts steering crash maneuvering, the track of the controlled vehicle resembles a quantic polynomial:

$$y = 10\frac{w}{r^3}x^3 + 15\frac{w}{r}x^4 + 6\frac{w}{r^5}x^5, \qquad (7)$$

$$r = x_{n+1} - x_n, \qquad (8)$$

$$w = y_{n+1} - y_n, \qquad (9)$$

where $x$ and $y$ represent the vertical and lateral coordinates of the vehicle riding on the planned path, respectively, and $r$ the distance the vehicle needs to ride to avoid a crash with the target vehicle (Zhu *et al.*, 2015).

We can achieve vehicle turning path planning using Eqs. (7)–(9). In addition, according to Zhu *et al.* (2015), the riding stability of the vehicle can be guaranteed when the lateral acceleration $|a_y| \leq 7$ m/s$^2$. In this case, we chose this value as the limit of lateral acceleration.

## 3  Experimental design and results

### 3.1  Experimental design

In this study, PRESCAN-MATLAB/SIMULINK joint simulation was used to construct a CCAS test environment. To reflect physical circumstances, a set of automobiles comprising two vehicles equipped with CCAS was used for the test (Kim *et al.*, 2016). Parameters for the test vehicles are listed in Table 1.

**Table 1  Vehicle dynamics constraints**

| Constraint | Value |
|---|---|
| Lateral acceleration limit, $a_y$ | $|a_y| \leq 7$ m/s$^2$ |
| Minimum acceleration, $g_{min}$ | 0.30 m/s$^2$ |
| Maximum acceleration, $g_{max}$ | 1.00 m/s$^2$ |

In the case where diverse initial cruising speeds were set for the two vehicles, kinetics control performances of the CCAS were tested under states of high and low speeds. The corresponding test scenarios are as follows:

**Scenario 1**    The test vehicle cruised with different initial speeds of 11 and 22 m/s. Collision with a target vehicle traveling in the same direction was imitated. To avoid such a collision, the CCAS checked the brake state in line with the real-time kinetics data of the target vehicle acquired by the DSRC module (Mirfakhraie *et al.*, 2014).

**Scenario 2**   The initial cruise speeds of the test vehicle were changed to 14 and 26 m/s. If it is possible that a collision with the target vehicle traveling in the same direction occurs, only checking brake cannot avoid such a collision, because the speed of the test vehicle is far higher than that of the target vehicle. If adjacent lanes allow secure lane variation, a maneuvering of a lane change with deceleration should be taken to avoid collision.

PID controllers with and without optimization were separately employed in the above scenarios to verify whether the improved PSO enables the CCAS to combine the braking intervention judgment module and turning path programming module in a more effective manner and achieve the goals of improved vehicle dynamic performance and fuel economy. To test the effects of the CCAS, a variable motion was set for the target vehicle during the experiments.

In the case where the vehicle takes advantage of a checking brake to avoid colliding with the target vehicle, the major factor affecting the stability and comfort of vehicles is their longitudinal acceleration. On this basis, longitudinal velocity and acceleration were collected. In addition, tier longitudinal displacement describing the behavior of the vehicle was recorded for scenario 1. When the vehicle undertakes a deceleration steering maneuver to avoid colliding with the target vehicle, its lateral acceleration is the primary factor affecting its dynamic stability. To portray the behavior of the vehicle in scenario 2, its transverse velocity and acceleration, wheel steering angle, and tier longitudinal displacement were collected (Wang *et al.*, 2015). Studies indicate that, on the premise of safety, a reduction in braking frequency and pressure is beneficial for reducing fuel consumption. To show that the method presented in this study contributes to fuel economy improvement, data associated with the brake pedal were acquired in scenario 2.

### 3.2  Results

Fig. 2 shows the velocity changes of the two vehicles in scenario 1. For convenience of analysis, velocities between 0 and 5500 s were shown. Figs. 2a and 2b show the results from the test vehicle operating at high and low speeds, respectively. Fig. 3 shows the acceleration of the test vehicle under low-speed cruising corresponding to Fig. 2a. A comparison be-

tween these two figures shows similar trends in variation, confirming the validity of our method (Yu *et al.*, 2016). Fig. 4 shows the longitudinal displacements of the wheels during deceleration to avoid colliding with the target vehicle in scenario 1, when the vehicle was cruising at an initial velocity of 11 m/s.
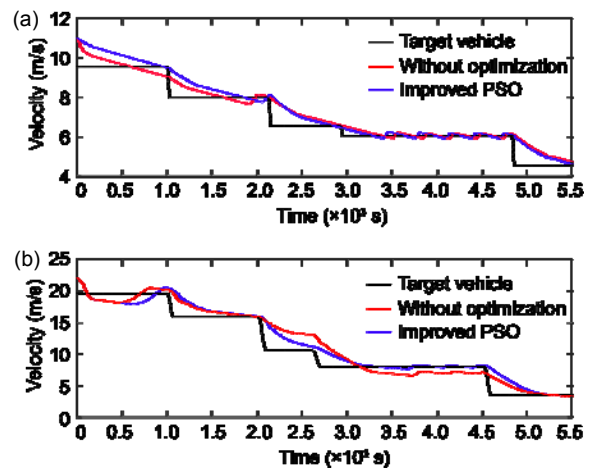


**Fig. 2  Vehicle velocities for scenario 1: (a) low initial speed; (b) high initial speed (Reference to color refer to the online version of this figure)**
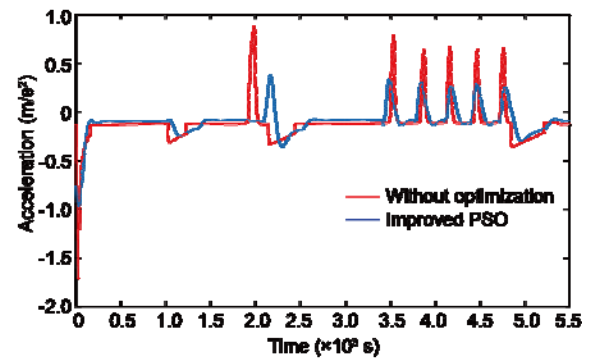


**Fig. 3  Acceleration of the test vehicle in scenario 1 with a low initial speed (References to color refer to the online version of this figure)**

To prove that the optimized PID controller in this study can improve the fuel economy performance of a vehicle equipped with CCAS, the pedal braking pressures of the vehicle during high- and low-speed cruising were recorded (Fig. 5). The blue curves represent the pressures of the test vehicle's brake pedal with the controller optimized by the proposed method, and the red curves represent the pressures of the test vehicle's brake pedal with the original controller. Clearly, the overall values of the red curves are
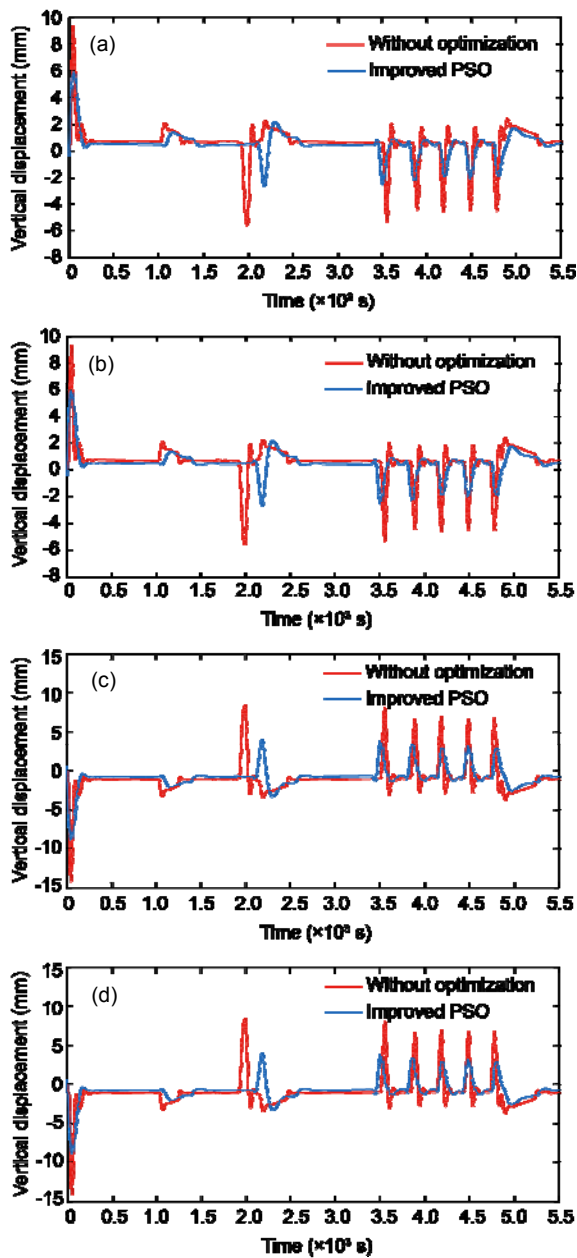
**Fig. 4 Vertical displacements of wheels in scenario 1 with a low initial speed: (a) left front wheel; (b) right front wheel; (c) left rear wheel; (d) right read wheel (References to color refer to the online version of this figure)**
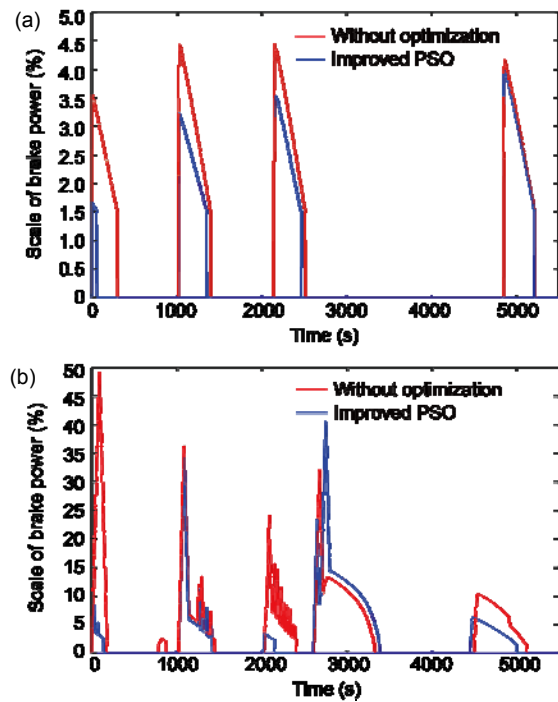


**Fig. 5 Scale of the brake power of the test vehicle in scenario (longitudinal running): (a) low initial speed; (b) high initial speed (References to color refer to the online version of this figure)**
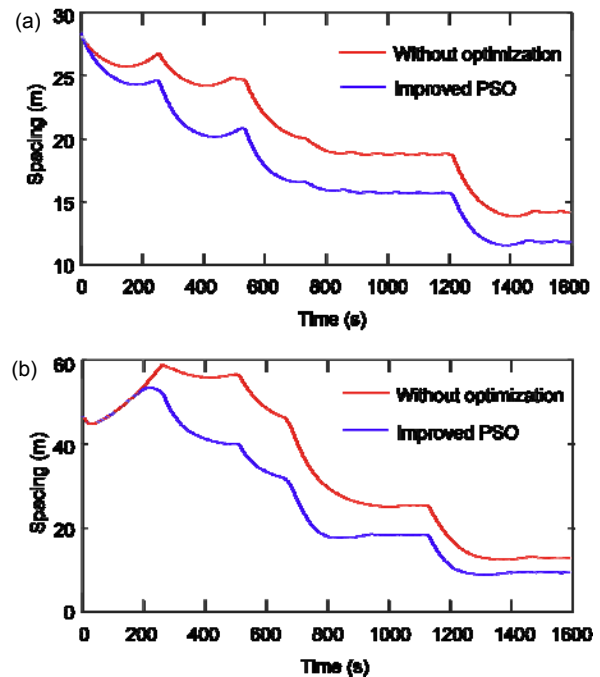


**Fig. 6 Vehicle spacing in scenario 1: (a) low initial speed; (b) high initial speed (References to color refer to the online version of this figure)**

higher than those of the blue curves, except for some particular time points. In addition, the slopes of the blue curves are smaller than those of the red curves.

Fig. 6 shows the in-situ distance between the test vehicle and the target vehicle when using deceleration braking to avoid collision in test scenario 1. As shown, the test vehicle in our simulation can avoid collision

with the target vehicle to different degrees with and without the optimization of the CCAS.

If a vehicle traveling at a high speed has passed the last possible point where braking would have an effect, it may still be possible to avoid an accident through steering, or taking evasive action (CAN Newsletter Online, 2014). In scenario 2, the velocity of the test vehicle was much higher than that of the target vehicle. Therefore, deceleration steering maneuvering was adopted to avoid collision. In this case, the main factor influencing vehicle stability is the transverse acceleration of the vehicle. We collected transverse velocity (Fig. 7) and acceleration (Fig. 8) of the test vehicle to assess its dynamic stability (Konstantinidis *et al.*, 2010).
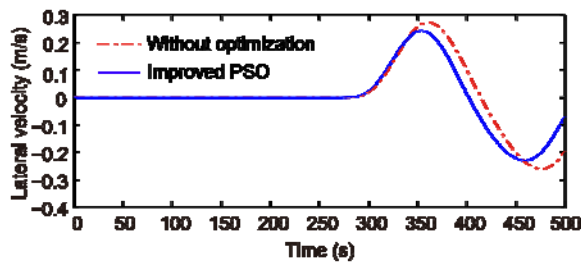


**Fig. 7  Lateral velocity of steering travel in scenario 2 with a low initial speed (References to color refer to the online version of this figure)**
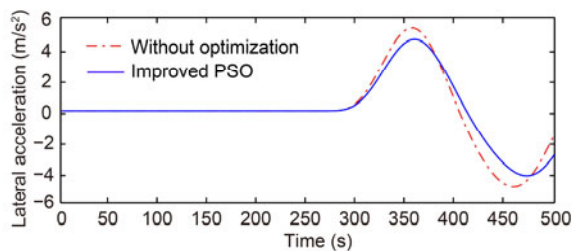


**Fig. 8  Lateral acceleration of steering travel in scenario 2 with a low initial speed (References to color refer to the online version of this figure)**

The change in the angle of the steering wheel can influence and describe the dynamic stability of a vehicle during steering maneuvering to a certain degree. Therefore, the steering wheel angle of the vehicle during high speed cruising at an initial speed of 26 m/s was recorded (Fig. 9). The blue curve in Fig. 10 represents the steering wheel angle generated when the controller was optimized by the proposed method, and the red curve represents the steering wheel angle generated when the controller was not
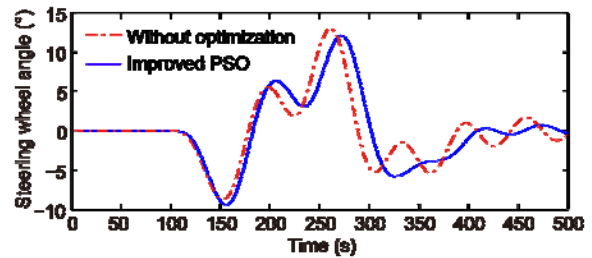


**Fig. 9  Steering wheel angle of steering travel in scenario 2 with a high initial speed (References to color refer to the online version of this figure)**

optimized. The trend in the variation of the blue curve was more stable than that of the red curve.

For quantitative analysis of the dynamic stability of the test vehicle when adopting deceleration steering maneuvering during high-speed cruising, we collected the longitudinal displacement of the wheels in scenario 2 (Fig. 10).

## 4  Discussion

In this study, we focused on improving the dynamic stability of a vehicle equipped with a CCAS. In this section we emphasize the experimental results which show that the optimized PID controller can better match the maneuver strategy judgement module and the turning path planning module, eventually improving the performance of CCAS.

Braking is effective for preventing a collision with the target vehicle when the test vehicle approaches with a speed slightly higher than that of the target vehicle. In this scenario, the main factors influencing the dynamic stability of the vehicle are its speed and acceleration. In Fig. 2a, the velocity of the target vehicle (black curve) remains constant between 0 and 100 s, while that of the test vehicle (blue and red curves) decreases. However, the slope of the red curve (test vehicle without optimization) is larger than that of the blue curve (test vehicle with optimization). In addition, the red curve shows a larger drop than the blue curve. These results indicate that, when a possible collision with the target vehicle is detected, CCAS can decelerate the vehicle no matter whether its PID controller is optimized or not. However, the optimized PID controller can better control the change of the test vehicle speed. In Fig. 2b, the rising trend of the blue curve is gentler than that of the red curve
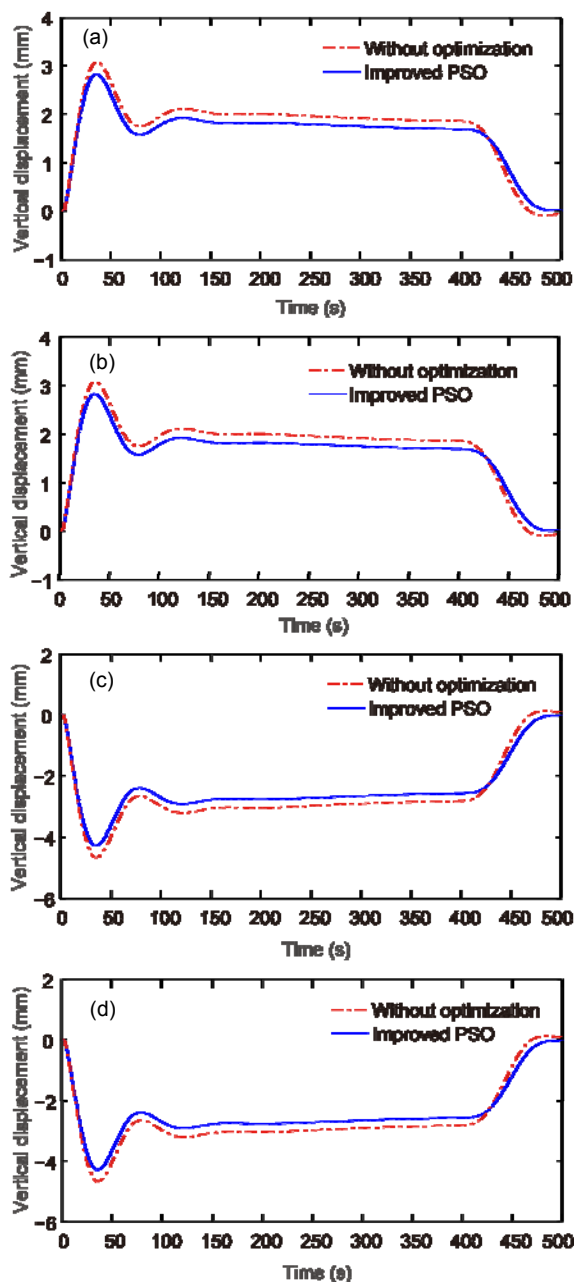
**Fig. 10 Vertical displacement of wheels during steering travel in scenario 2 with a high initial speed: (a) left front wheel; (b) right front wheel; (c) left rear wheel; (d) right rear wheel (References to color refer to the online version of this figure)**

between 500 and 1000 s. Both the blue and red curves decline as the black curve declines between 1000 and 1500 s, but the blue curve has clearly a smaller slope (Zhang *et al.*, 2012). A similar effect can be observed between 2000 and 3000 s. These results indicate that the PID controller of a CCAS, after being optimized,

can better control the velocity of a vehicle based on the speed of the target vehicle, thereby to some extent improving the riding stability and comfort of the vehicle equipped with CCAS.

As shown in Fig. 3, both the blue and red curves underwent a rapid drop followed by a rapid rise between 0 and 200 s, which is consistent with the situation in Fig. 2a. In addition, the drop and rise of the blue curve are significantly smaller than those of the red curve. In comparison with Fig. 2a, both the blue and red curves fluctuate between 1000 and 3000 s, but the amplitude of fluctuation of the blue curve is significantly smaller than that of the red curve. In Fig. 2a, the blue curve and red curve show a continuous change of speed between 3500 and 4800 s. The two curves show similar fluctuations in Fig. 3, but it is obvious that the change in the blue curve is more gentle than that in the red curve. These results indicate that the PID controller optimized by the proposed method can help a CCAS better control the change in a vehicle's acceleration and improve its riding stability while preventing a collision with the target vehicle. The appendix shows the relationship between vehicle acceleration and the passangers' comfort reported by Wu and Lu (2009). Accordingly, in Fig. 3, the peak value of the blue curve is smaller than 1 m/s$^2$, and the peak value of the red curve is larger than 1.5 m/s$^2$. These results indicate that the PID controller optimized by the proposed method can significantly improve the riding comfort of a vehicle with a CCAS. Furthermore, the results in Figs. 2 and 3 are consistent with those of Wu and Lu (2009).

In Fig. 4a, both the blue and red curves fluctuate significantly between 0 and 400 s, but the peak value of the blue curve is significantly smaller than that of the red curve. This result is consistent with the situation in Fig. 3. Compared with the red curve, the blue curve changes in a more linear way, but within a narrower range between 1000 and 1500 s. Similar to Fig. 3, five consecutive fluctuations occur between 3400 and 5000 s in Fig. 4a (Khan *et al.*, 2015). Note that the range of variation in the blue curve is always smaller than that in the red curve. These results indicate that the optimized PID controller of CCAS can achieve the objective of this study, i.e., to improve the riding stability and comfort of a vehicle with a CCAS, since it can better control the vehicle's change of acceleration.

Braking is a process in which the vehicle's kinetic energy is converted into heat energy and consumed when the wheels rub against the ground and brake pads. Therefore, energy consumption can be reduced by reducing the brake pressure and frequency of braking, when not sacrificing safety. In Fig. 5a, the peak value and slope of the blue curve are smaller than their counterpart of the red curve, suggesting that the optimized PID controller can better control the change in the vehicle's travel speed. Therefore, the vehicle can keep a safety distance from the target vehicle by exerting a smaller brake pressure. When the blue curve and red curve in Fig. 2b start to drop at some point, their counterparts in Fig. 5b start to rise, thus proving the validity of the data analyzed by Zhang *et al.* (2013). These results indicate that the PID controller of a CCAS, after being optimized by the proposed method, can control brake pressure in a more effective way to improve the vehicle's riding stability and fuel economy, without sacrificing safety.

For convenience of description, the distances between vehicles in the first 1600 s were extracted for analysis in Fig. 6. In Fig. 6a, both the blue and red curves drop between 0 and 100 s, since the initial speed of the test vehicle is larger than that of the target vehicle. The two curves show a rising trend between 100 and 250 s, indicating that the CCAS brakes the vehicle when it detects the possibility of a collision with the target vehicle, and the distance between the test vehicle and the target vehicle is thus increased. The red curve rises significantly, suggesting that the CCAS cannot control the change in travel speed well with its PID controller unoptimized. Moreover, the rapidly decreasing speed not only extends its distance from the target vehicle, but also influences the riding stability and comfort of the test vehicle. Compared with the red curve, the blue curve drops in a more linear way between 550 and 750 s. This shows that the optimized PID controller can not only prevent collision, but also manipulate the travel speed to drop linearly, thereby achieving the objective of the present study. In Fig. 6b, both the blue curve and red curve rise after a drop between 20 and 220 s, but it is obvious that the red curve continues to rise while the blue curve starts to drop after 200 s. Compared with the red curve, the blue curve drops more gently between 220 and 1000 s. These results indicate that the PID controller of a CCAS can prevent collision

with the target vehicle no matter whether it is optimized or not. However, the travel speed changes in a more linear way after the PID controller is optimized by the proposed method.

For ease of analysis, Fig. 7 presents the lateral velocity of the test vehicle in the initial 500 s during cruising at an initial speed of 14 m/s. Clearly, between 340 and 500 s, the peak of the blue curve is lower than that of the red curve. In addition, the blue curve has a smaller slope than the red curve during the descent. As discussed above, the optimized PID controller offers better control of velocity changes. Therefore, the transverse stability of the vehicle is improved.

In Fig. 8, the rising trend of the blue curve is gentler than that of the red curve between 300 and 350 s. In addition, the peak of the blue curve is lower than that of the red curve at 350 s. The two curves start to drop after 350 s. It is obvious that the blue curve drops more gently than the red curve. The literature reveals that occupants feel almost nothing during a normal acceleration of $a_n \leq 1.8$ m/s$^2$; they feel tolerably discomfortable when $a_n = 3.6$ m/s$^2$, and intolerably discomfortable when $a_n \geq 5.0$ m/s$^2$. Fig. 8 shows that the change of the blue curve is always within the range that is acceptable for occupants, while the change in the red curve exceeds that range. The results indicate that the PID controller of a CCAS can effectively control the change in traveling speed and improve the vehicle's lateral stability and riding comfort after being optimized by the proposed method.

In Fig. 9, the peak of the blue curve is higher than that of the red curve between 150 and 220 s, but lower than that of the red curve after 220 s. In addition, the amplitude of fluctuation of the blue curve is significantly smaller than that of the red curve between 300 and 500 s. These results indicate that the PID controller of a CCAS can better control the change in travel speed after it is optimized by the proposed method. The change in the steering wheel angle reflects better stability and linearity.

In Fig. 10, the blue and red curves fluctuate significantly in the first 40 s. In Figs. 10a and 10b, the peak of the blue curve is lower than that of the red curve; in Figs. 10c and 10d, the extreme value of the blue curve is larger than that of the red curve. Moreover, the slope where the blue curve reaches its extreme point is smaller than that of the red curve.

The curves in Fig. 10 fluctuate continuously between 30 and 150 s, but the blue curve changes more gently than the red curve. After 440 s, the two curves approach zero, but the blue curve changes more gently than the red curve. These results indicate that, under the condition in which collision can be avoided, the optimized CCAS control unit can partly optimize the vehicle's riding stability and thereby improve its riding comfort (Chen and Chou, 2013).

## 5 Conclusions

The introduction of PID controllers into CCAS has some inherent problems. For example, the PID controller cannot be optimized rationally, and our understanding of its possible effects on stability, comfort, and fuel economy for vehicles is insufficient. In response to these issues, an improved PSO algorithm was adopted in this study to optimize a PID controller. With this method, a CCAS can fulfill the dynamic control over vehicles in a more favorable way. To improve the convergence property of the algorithm and obtain the global optimum of the problem, a stochastic inertia weight and an incidental learning factor are incorporated in the improved PSO with worst positions for individual particles and the swam. On one hand, the diversity of the particle swarm is enriched; on the other hand, the algorithm can be prevented from falling into local optima. To verify that the proposed method can enhance the stability under transport conditions and can improve the comfort and fuel economy of vehicles equipped with CCAS, two experimental scenarios were simulated and the required automobile dynamics data collected. Through analysis of the relevant data, the PID controller optimized by the proposed method was shown to be able to match the braking intervention judgment module and the turning path programming module, and finally to intensify the handling performance of CCAS. In the future, we will focus on finding solutions to hysteretic responses and other problems of CCAS.

## References

CAN Newsletter Online, 2014. Emergency Steering Assist. http://can-newsletter.org/engineering/engineering-miscel laneous/140813_emergency-steering-assist

Chen, L.W., Chou, P.C., 2013. A lane-level cooperative colli- sion avoidance system based on vehicular sensor net- works. 19th Annual Int. Conf. on Mobile Computing & Networking, p.131-134. https://doi.org/10.1145/2500423.2505293

Cho, H., Kim, B., 2014. Cooperative intersection collision- warning system based on vehicle-to-vehicle communica- tion. *Contemp. Eng. Sci.*, **7**(22):1147-1154. https://doi.org/10.12988/ces.2014.49143

Feng, Y.Q., Ji, H.Q., Liu, Z.S., 2012. Parameter setting and simulation of the PID controller for vehicle spacing con- trol system. *China Sci. Technol. Inform.*, **2012**(8):141- 143 (in Chinese).

Huang, C.M., Lin, S.Y., 2014. Cooperative vehicle collision warning system using the vector-based approach with dedicated short range communication data transmission. *IET Intell. Transp. Syst.*, **8**(2):124-134. https://doi.org/10.1049/iet-its.2012.0101

Jin, C., Wang, J., Ma, J., et al., 2010. Application of improved PSO for parameter tuning of PID controller. *J. Electron. Meas. Instrum.*, **24**(2):141-146. https://doi.org/10.3724/SP.J.1187.2010.00141

Khan, H., Iqbal, J., Baizid, K., et al., 2015. Longitudinal and lateral slip control of autonomous wheeled mobile robot for trajectory tracking. *Front. Inform. Technol. Electron. Eng.*, **16**(2):166-172. https://doi.org/10.1631/FITEE.1400183

Kim, K.I., Guan, H., Wang, B., et al., 2016. Active steering control strategy for articulated vehicles. *Front. Inform. Technol. Electron. Eng.*, **17**(6):576-586. https://doi.org/10.1631/FITEE.1500211

Konstantinidis, E.I., Patoulidis, G.I., Vandikas, I.N., et al., 2010. Development of a collaborative vehicle collision avoidance system. IEEE Intelligent Vehicles Symp., p.1066-1071. https://doi.org/10.1109/IVS.2010.5548022

Kreuzen, C., 2012. Cooperative Adaptive cruise control using information from multiple predecessors in combination with MPC. MS Thesis, Delft University of Technology, Delft, the Netherlands.

Lee, D.H., Bai, S.N., Kim, T.W., et al., 2010. Enhanced se- lective forwarding scheme for alert message propagation in VANETs. Int. Conf. on Information Science and Ap- plications, p.1-9. https://doi.org/10.1109/ICISA.2010.5480516

Mirfakhraie, T., He, Y., Liscano, R., 2014. Wireless networked control for active trailer steering systems of articulated vehicles. ASME Int. Mechanical Engineering Congress and Exposition, Volume 12: Transportation Systems, p.V012T15A003. https://doi.org/10.1115/IMECE2014-36440

Ong, H.Y., Gerdes, J.C., 2015. Cooperative collision avoid- ance via proximal message passing. American Control Conf., p.4124-4130. https://doi.org/10.1109/ACC.2015.7171976

Seo, H.S., Jung, J.S., Lee, S.S., 2014. Network performance analysis and manuever model for overtaking assistant service using wave. *Int. J. Autom. Technol.*, **15**(1):57-64. https://doi.org/10.1007/s12239-014-0006-x

Shi, Y., Eberhart, R., 1998. A modified particle swarm optimizer. IEEE Int. Conf. on Evolutionary Computation, p.69-73. https://doi.org/10.1109/ICEC.1998.699146

Shi, Y., Eberhart, R.C., 2001. Fuzzy adaptive particle swarm optimization. Congress on Evolutionary Computation, p.101-106. https://doi.org/10.1109/CEC.2001.934377

Solyom, S., Bengtsson, M., 2012. Collision Avoidance System in a Vehicle. US Patent 8 200 420.

Tan, H.S., Huang, J., 2006. DGPS-based vehicle-to-vehicle cooperative collision warning: engineering feasibility viewpoints. *IEEE Trans. Intell. Transp. Syst.*, **7**(4):415-428. https://doi.org/10.1109/TITS.2006.883938

Wang, Q., Phillips, C., 2013. Cooperative collision avoidance for multi-vehicle systems using reinforcement learning. 18th Int. Conf. on Methods & Models in Automation & Robotics, p.98-102.
https://doi.org/10.1109/MMAR.2013.6669888

Wang, Q., Zhu, S., He, Y., 2015. Model reference adaptive control for active trailer steering of articulated heavy vehicles. SAE Technical Papers, 2015-01-1495.
https://doi.org/10.4271/2015-01-1495

Wang, Q.G., Zou, B., Lee, T.H., *et al.*, 1997. Auto-tuning of multivariable PID controllers from decentralized relay feedback. *Automatica*, **33**(3):319-330.
https://doi.org/10.1016/S0005-1098(96)00177-X

Wu, Y.H., Lu, Y.P., 2009. Main factors and evaluation methods of driving comfort. *Heilongjiang Jiaotong Keji*, **2009**(8): 197-198 (in Chinese).
https://doi.org/10.16402/j.cnki.issn1008-3383.2009.08. 107

Yan, G., Yang, W., Weigle, M.C., *et al.*, 2010. Cooperative collision warning through mobility and probability prediction. IEEE Intelligent Vehicles Symp., p.1172-1177. https://doi.org/10.1109/IVS.2010.5547990

Yu, C.B., Wang, Y.Q., Shao, J.L., 2016. Optimization of formation for multi-agent systems based on LQR. *Front. Inform. Technol. Electron. Eng.*, **17**(2):96-109.
https://doi.org/10.1631/FITEE.1500490

Zardosht, B., Beauchemin, S., Bauer, M.A., 2013. A decision making module for cooperative collision warning systems using vehicular ad-hoc networks. 16th Int. IEEE Conf. on Intelligent Transportation Systems, p.1743-1749. https://doi.org/10.1109/ITSC.2013.6728481

Zhang, H.T., Hu, H.L., Wang, B., 2008. A modified PSO algorithm and its application in tuning of PID. *Techn. Autom. Appl.*, **27**(12):14-16.
https://doi.org/10.3969/j.issn.1003-7241.2008.12.004

Zhang, J.M., Li, Q., Cheng N., *et al.*, 2013. Nonlinear path-following method for fixed-wing unmanned aerial vehicles. *J. Zhejiang Univ.-Sci. C (Comput. & Electron.)*, **14**(2):125-132. https://doi.org/10.1631/jzus.C1200195

Zhang, M.H., Duan, D.P., Chen, L., 2012. Turning mechanism and composite control of stratospheric airships. *J. Zhejiang Univ.-Sci. C (Comput. & Electron.)*, **13**(11): 859-865. https://doi.org/10.1631/jzus.C1200084

Zhu, X., Liu, Z., Li, L., 2015. Evasive manoeuvre for emergency steering based on typical vehicle-pedestrian use case. *J. Autom. Safety Energy*, **6**(3):217-223 (in Chinese). https://doi.org/10.3969/j.issn.1674-8484.2015.03.003

## Appendix: Relationship between vehicle acceleration and human subjective comfort

According to Wu and Lu (2009), when a vehicle's acceleration is between 0.315 and 1 m/s$^2$, an occupant feels basically comfortable, whereas when the acceleration is larger than 1.5 m/s$^2$, an occupant feels very uncomfortable. The relationship between vehicle acceleration and human subjective comfort is shown in Table A1.

**Table A1   Relationship between vehicle acceleration and human subjective comfort (Wu and Lu, 2009)**

| Weighted acceleration (m/s$^2$) | Passenger subjective feeling |
| --- | --- |
| <0.315 | Not discomfortable |
| 0.315–0.630 | Slightly discomfortable |
| 0.500–1.000 | Somewhat discomfortable |
| 0.800–1.600 | Discomfortable |
| 1.250–2.500 | Very discomfortable |
| >2.000 | Extremely discomfortable |